

Enhancement of the color quality scale of white LEDs using red-emitting $\text{Sr}_w\text{F}_x\text{B}_y\text{O}_z:\text{Eu}^{2+}, \text{Sm}^{2+}$ phosphor

N. D. Q. ANH^{a,*}, P. X. LE^{b,*}, H. Y. LEE^{c,*}

^aFaculty of Electrical & Electronics Engineering, Ton Duc Thang University, Ho Chi Minh City, Vietnam

^bFaculty of Electrical and Electronics Engineering, HCMC University of Food Industry, Ho Chi Minh city, Vietnam

^cDepartment of Electrical Engineering, National Kaohsiung University of Applied Sciences, Kaohsiung City, Taiwan

In this paper, the red-emitting $\text{Sr}_w\text{F}_x\text{B}_y\text{O}_z:\text{Eu}^{2+}, \text{Sm}^{2+}$ phosphor is proposed to enhance the color quality scale (CQS) of multi-chip white LEDs (WLEDs) in two configurations, conformal phosphor and in-cup phosphor. Because of the compensation of red-light spectrum band, the CQS can be improved to a greater value than 76. Moreover, the effects of the $\text{Sr}_w\text{F}_x\text{B}_y\text{O}_z:\text{Eu}^{2+}, \text{Sm}^{2+}$ phosphor on the attenuation of light are also verified based on the Lambert-Beer law and Mie-scattering theory. The obtained result is as an important instruction which can contribute to the fabrication of WLEDs with higher CQS.

(Received September 21, 2017; accepted February 12, 2018)

Keywords: White LEDs, Lambert-Beer law, Mie-scattering theory, Color quality scale, Luminous efficacy

1. Introduction

In recent years, there are remarkable efforts in developing white light-emitting diodes (WLEDs) by the promising illumination method to replace the traditional lighting sources due to their superior features, such as small energy consumption, lengthy life span and variable color [1-4]. Consequently, WLEDs have been actively developed and required a higher color rendering index (CRI) for lighting applications [5, 6]. The conventional WLEDs involves a combination of nine blue LEDs with the yellow YAG:Ce³⁺ phosphor compounding. However, because of lacking in the component of red-light, which leads to poor color rendering ability (less than 74). Recently, there has been tendency in combining the quantum dot nanophosphor and the warm-white LEDs in order to increase CRI close to 90 at correlated color temperature (CCT) less than 3000 K [7]. It was shown that WLEDs with CCT from 2700 K to 4700 K and CRI value 85.6 can be accomplished by using a pulse-sprayed conformal phosphor configuration [8]. Besides, a new tool has been created and developed for practical LED system designers in order to calculate the instantaneous variation in CCT and CRI when the LED system power varies. In 2016, the CeTb green phosphor was used to improve the color uniformity and the luminous efficacy of multi-chip white LED lamps, but that makes the color rendering ability decreases significantly [9]. Indeed, the above mentioned works also proposed the methods to improve luminous efficacy (LE) and CRI. However, the result is not enough ideal for illumination applications. Moreover, those studies only pay attention to research single-chip white LED lamps. Thus, how to maintain the good balance between the values of CRI and LE is critical for producing WLED packages, and that's the reason why it should be

addressed rigorously. In several recent studies [10, 11], scientists have taken the color quality scale (CQS) so that overall color quality could be estimated. The CQS incorporates important modifications to overcome the imperfection of CRI and concentrates on a broader definition of color quality such as CRI, chromatic discrimination, and observer preferences [12].

$\text{Sr}_w\text{F}_x\text{B}_y\text{O}_z:\text{Eu}^{2+}, \text{Sm}^{2+}$, which is a Eu-sensitized, red-emitting with high efficient phosphor, has been widely employed in high and low-pressure discharge lamps due to its advantage of excellent thermal and chemical stability [13-17]. However, $\text{Sr}_w\text{F}_x\text{B}_y\text{O}_z:\text{Eu}^{2+}, \text{Sm}^{2+}$ is seldom applied in kind of these studies to make the CQS of WLEDs get better up to now. In this research, $\text{Sr}_w\text{F}_x\text{B}_y\text{O}_z:\text{Eu}^{2+}, \text{Sm}^{2+}$ is proposed to enhance CQS. This can be obtained by supplementing deficiency-red-light. Moreover, by means of the Lambert-Beer law and Mie theory as well as Monte Carlo simulation, we demonstrate that both the concentration and particle size of $\text{Sr}_w\text{F}_x\text{B}_y\text{O}_z:\text{Eu}^{2+}, \text{Sm}^{2+}$ have significantly impact on the transmitted light power. Therefore, we are able to keep the good balance of CQS and LE values regardless of phosphor configurations or higher CCTs.

2. Experimental details

2.1. Optical model

The optical models of WLEDs are constructed basing on its measured parameters as displayed in Fig. 1. The simulation process on various WLED configurations is carried out via using the commercial software package LightTools. This process comprises the setup of conformal phosphor (CPC) and in-cup phosphor configuration (IPC)

with the same average CCT of 8500 K in order to guarantee that our simulation results reflect precisely the impact of considered parameters. The absorption, excitation and emission spectra of $\text{Sr}_w\text{F}_x\text{B}_y\text{O}_z:\text{Eu}^{2+}, \text{Sm}^{2+}$ are first set in LightTools program. The concentration and size of $\text{Sr}_w\text{F}_x\text{B}_y\text{O}_z:\text{Eu}^{2+}, \text{Sm}^{2+}$ are varied to figure out suitable values for optical properties of WLEDs. The added concentration of $\text{Sr}_w\text{F}_x\text{B}_y\text{O}_z:\text{Eu}^{2+}, \text{Sm}^{2+}$ ranges from 0 to 16 % for CPC. Meanwhile, that of IPC only varies from 0 to 0.32 %. There is a significant deviation between the added $\text{Sr}_w\text{F}_x\text{B}_y\text{O}_z:\text{Eu}^{2+}, \text{Sm}^{2+}$ concentration values for those 2 cases due to their different phosphor configurations. Secondly, the other factors such as LED's wavelength, waveform, light intensity, and operating temperature are also set for the actual WLEDs to construct the precise WLED models. This model presents the best optical-thermal stability, hence, it can minimize the variations caused by uninteresting parameters.



Fig. 1. The experimental WLED having CCT of 8500 K

The absorption, excitation and emission spectra, which are presented in Fig. 2, are considered to simulate $\text{Sr}_w\text{F}_x\text{B}_y\text{O}_z:\text{Eu}^{2+}, \text{Sm}^{2+}$ phosphor. Its particles emit the strong red light at 684 nm under UV light (254 nm), while $\text{Sr}_w\text{F}_x\text{B}_y\text{O}_z:\text{Eu}^{2+}, \text{Sm}^{2+}$ phosphor exhibits a rather weak emission under blue (453 nm) or yellow-green light (555 nm). Thus, it can be expected that such combination would exhibit a low luminous efficiency due to poor excitation (250-280 nm and 300-390 nm) of $\text{Sr}_w\text{F}_x\text{B}_y\text{O}_z:\text{Eu}^{2+}, \text{Sm}^{2+}$ phosphors. This is the reason why that Sm^{2+} ion is added to $\text{Sr}_w\text{F}_x\text{B}_y\text{O}_z:\text{Eu}^{2+}, \text{Sm}^{2+}$, resulting in additional peaks at 395, 420 and 502 nm. The measured emission intensity of $\text{YAG}:\text{Ce}^{3+}$ phosphor at 502 nm is approximately equal to 1/2 that of at 555 nm. In that case there will be the slight loss of luminous efficiency due to the reabsorption. It is more important that two excitation peaks of 420 nm and 502 nm are suitable for the emission band of the used blue chip at 416-516 nm.

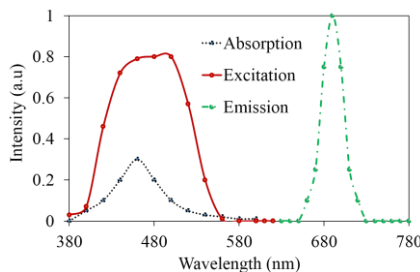


Fig. 2. Absorption, excitation and emission spectra of $\text{Sr}_w\text{F}_x\text{B}_y\text{O}_z:\text{Eu}^{2+}, \text{Sm}^{2+}$ phosphor

Both CPC and IPC also applied the identical silicone lens and construction to make the comparison fair. Specifically, we set respectively the depth, inner and outer radius of reflector approximately to 2 mm, 4 mm, and 5 mm. Nine LED chips are covered by either CPC or IPC, which respectively have fixed thickness of 0.08 mm and 2.07 mm. Each blue chip has a size of 1.14 mm by 0.15 mm, the radiant flux of 1.16 W, and the peak wavelength of 453 nm. These configuration is intentionally set similar to the one in our previous study [5]. In order to maintain the same color of WLEDs when either the concentration or the size of $\text{Sr}_w\text{F}_x\text{B}_y\text{O}_z:\text{Eu}^{2+}, \text{Sm}^{2+}$ particles varies, the $\text{YAG}:\text{Ce}^{3+}$ phosphor concentration should be inversely changed to provide the same CCT value.

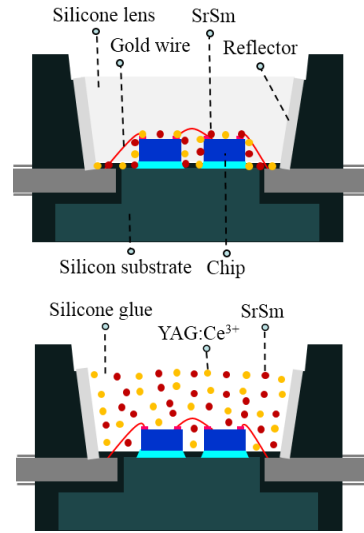


Fig. 3. Illustration of WLEDs with (top) the conformal phosphor configuration (CPC); (bottom) the in-cup phosphor configuration (IPC)

Fig. 3(a) shows that the phosphor layer of CPC is coated conformally on 9 LEDs, while in Fig. 3(b), the phosphor particles of IPC is dispersed in the silicone lens. These phosphor films consist of $\text{YAG}:\text{Ce}^{3+}$ and $\text{Sr}_w\text{F}_x\text{B}_y\text{O}_z:\text{Eu}^{2+}, \text{Sm}^{2+}$ particles as well as the silicone glue, which respectively have the refractive indices of 1.83, 1.93 and 1.5. In addition, the particle size is also a critical element to expand the optical properties. Here, the ordinary radius of $\text{YAG}:\text{Ce}^{3+}$ phosphor particles is set to 7.25 μm for all packages, which size is exactly the same value of a real particle. Moreover, the molar percentage of each element of $\text{Sr}_w\text{F}_x\text{B}_y\text{O}_z:\text{Eu}^{2+}, \text{Sm}^{2+}$ phosphor is calculated basing on its compositions [13]. The detailed description of the red-emitting $\text{Sr}_w\text{F}_x\text{B}_y\text{O}_z:\text{Eu}^{2+}, \text{Sm}^{2+}$ phosphor is presented in Table 1.

2.2. Computation of scattering

The Lambert-Beer law [18] can be applied to derive the relationship between luminous efficacy and the $\text{Sr}_w\text{F}_x\text{B}_y\text{O}_z:\text{Eu}^{2+}, \text{Sm}^{2+}$ weight rigorously. The transmitted light power can be calculated by

$$I = I_0 \exp(-\mu_{ext}L) \quad (1)$$

This formula describes I_0 as the incident light power, while L is the phosphor layer thickness (mm) and μ_{ext} is the extinction coefficient, which can be expressed as

$\mu_{ext} = N_r \cdot C_{ext}$, in here N_r is the density spreading of particles (mm^{-3}). C_{ext} is the extinction cross-section (mm^2), which is defined by the equation 2.

Table 1. The chemical compositions of $\text{Sr}_w\text{F}_x\text{B}_y\text{O}_z:\text{Eu}^{2+}, \text{Sm}^{2+}$ phosphor

Ingredient	Mole (%)	By weight (g)	Molar mass (g/mol)	Mole (mol)	Ions	Mole (mol)	Mole (%)	
$\text{Sr}(\text{NO}_3)_2$	10.09	126.98	211.63	0.6	Sr^{2+}	0.6	w	0.0241
SrF_2	5.43	40.58	125.62	0.32	F^-	0.646	x	0.0259
H_3BO_3	84.12	309.2	61.83	5	B^{3+}	5	y	0.203
Eu_2O_3	0.25	5.28	351.93	0.015	O^{2-}	18.665	z	0.748
Sm_2O_3	0.11	2.09	348.72	0.006	Eu^{2+}	0.03		0.0012
$\text{Sr}_w\text{F}_x\text{B}_y\text{O}_z:\text{Eu}^{2+}, \text{Sm}^{2+}$					Sm^{2+}	0.012		0.00048

$$C_{ext} = \frac{2\pi a^2}{x^2} \sum_{n=1}^{\infty} (2n+1) \text{Re}(a_n + b_n) \quad (2)$$

Here $x = 2\pi a/\lambda$ is the size parameter, a_n and b_n are respectively the extension coefficients with even and odd symmetry. The distinct wavelengths of 453 nm and 555 nm are used to determine the extinction coefficient of $\text{Sr}_w\text{F}_x\text{B}_y\text{O}_z:\text{Eu}^{2+}, \text{Sm}^{2+}$ corresponding to the emission peaks of LED chips and $\text{YAG}:\text{Ce}^{3+}$, $\text{Sr}_w\text{F}_x\text{B}_y\text{O}_z:\text{Eu}^{2+}, \text{Sm}^{2+}$ phosphors. With the thickness of phosphor layer for CPC, IPC, the number density distribution of particles N_r and the extinction cross-section C_{ext} are functions of the concentration and particle size of $\text{Sr}_w\text{F}_x\text{B}_y\text{O}_z:\text{Eu}^{2+}, \text{Sm}^{2+}$. Hence, transmitted light power I changes accordingly with these 2 parameters.

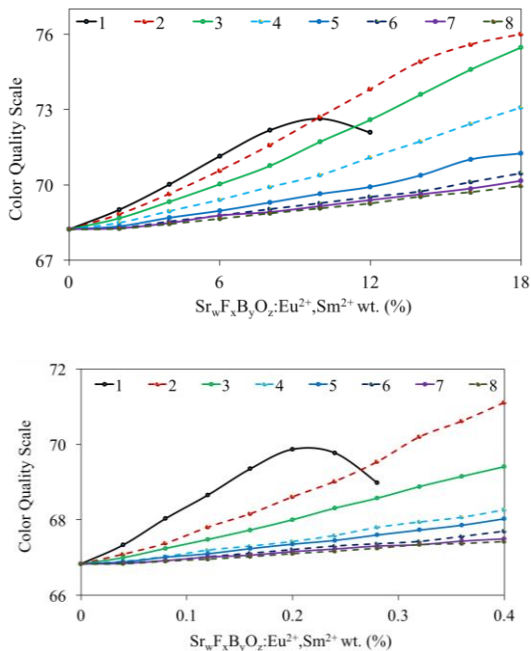


Fig. 4. Color quality scale of phosphor configurations corresponding to concentration (%) and size (μm) of $\text{Sr}_w\text{F}_x\text{B}_y\text{O}_z:\text{Eu}^{2+}, \text{Sm}^{2+}$: (top) CPC; (bottom) IPC

3. Results and discussions

In this section, CQS and LE values are presented as a function of size and concentration of $\text{Sr}_w\text{F}_x\text{B}_y\text{O}_z:\text{Eu}^{2+}, \text{Sm}^{2+}$. Firstly, the CQS's index can be seen through Fig. 4. Fig. 4(top) illustrates the influence of $\text{Sr}_w\text{F}_x\text{B}_y\text{O}_z:\text{Eu}^{2+}, \text{Sm}^{2+}$ concentration on CQS of CPC configuration. It can be easily find that the growth of CQS in accordance with the weight percentage of $\text{Sr}_w\text{F}_x\text{B}_y\text{O}_z:\text{Eu}^{2+}, \text{Sm}^{2+}$ phosphor continue ranging from 0% to nearly 10 % for all $\text{Sr}_w\text{F}_x\text{B}_y\text{O}_z:\text{Eu}^{2+}, \text{Sm}^{2+}$ particles. When the concentration of $\text{Sr}_w\text{F}_x\text{B}_y\text{O}_z:\text{Eu}^{2+}, \text{Sm}^{2+}$ varies from 12% to 18% in the 2-8 μm size region, CQS will get a higher quality. In particular, ideal color quality scale can be achieved exceeds 76 in this region. Indeed, the CQS tends to increase with the concentration of $\text{Sr}_w\text{F}_x\text{B}_y\text{O}_z:\text{Eu}^{2+}, \text{Sm}^{2+}$. Meanwhile, the LE increases with the size of $\text{Sr}_w\text{F}_x\text{B}_y\text{O}_z:\text{Eu}^{2+}, \text{Sm}^{2+}$ particles, as presented in Fig. 5. The extinction coefficients of the $\text{Sr}_w\text{F}_x\text{B}_y\text{O}_z:\text{Eu}^{2+}, \text{Sm}^{2+}$ particles have been calculated at the emission wavelength of 453 nm and 555 nm. Extinction is the sum of absorption and scattering. $\text{Sr}_w\text{F}_x\text{B}_y\text{O}_z:\text{Eu}^{2+}, \text{Sm}^{2+}$ is supposed to absorb both 453 nm and 555 nm and re-emit at 684nm. On the other hand, scattering cross-section increases with the particle size according to Mie scattering theory.

As for IPC configuration, the concentration of $\text{Sr}_w\text{F}_x\text{B}_y\text{O}_z:\text{Eu}^{2+}, \text{Sm}^{2+}$ uninterruptedly changes from 0% to approximately 0.4 %. The development of CQS can be obtained by the $\text{Sr}_w\text{F}_x\text{B}_y\text{O}_z:\text{Eu}^{2+}, \text{Sm}^{2+}$ percentage within the range from 0 to 0.2 % for all particle size, as shown in Fig. 4(bottom). The CQS continue to increase in the range of 0.2 to 0.4 % in the range of 2-8 μm . The optimal CQS of WLEDs can go beyond 71 in this circumstance, which is 6 % higher than that of the non- $\text{Sr}_w\text{F}_x\text{B}_y\text{O}_z:\text{Eu}^{2+}, \text{Sm}^{2+}$, meaning that when just having 0 % of concentration. However, the unbalance of color distribution of WLED will occur if concentration and particle size of $\text{Sr}_w\text{F}_x\text{B}_y\text{O}_z:\text{Eu}^{2+}, \text{Sm}^{2+}$ are increased outside a point where the red-light starts to be over-dominant. As a result, the

CQS tend to be significantly reduced. The performance of CPC, IPC are also described in Fig. 5, which shown the alike phenomenon with respect to the concentration and size of $\text{Sr}_w\text{F}_x\text{B}_y\text{O}_z:\text{Eu}^{2+},\text{Sm}^{2+}$. On one hand, the simulation confirms that CPC provides a better overall CQS than IPC does.

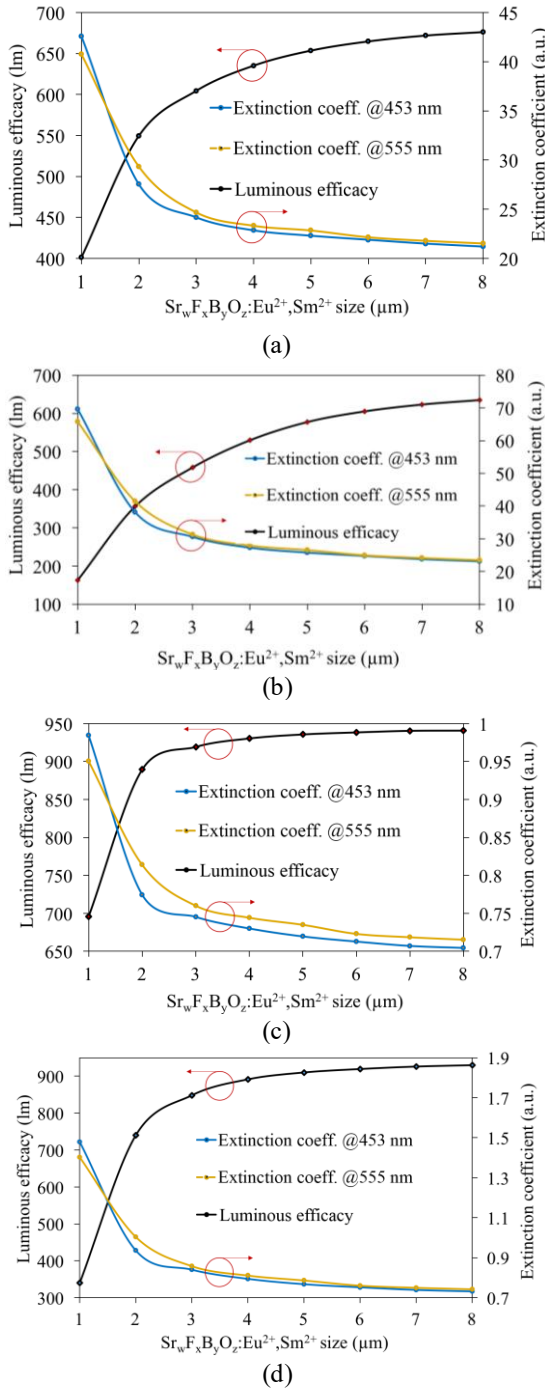


Fig. 5. Luminous efficacy and extinction coefficient of phosphor configurations corresponding to concentration and size of $\text{Sr}_w\text{F}_x\text{B}_y\text{O}_z:\text{Eu}^{2+},\text{Sm}^{2+}$: (a) CPC with 6 % wt. (b) CPC with 12 % wt. (c) IPC with 0.16 % wt. (d) IPC with 0.32% wt

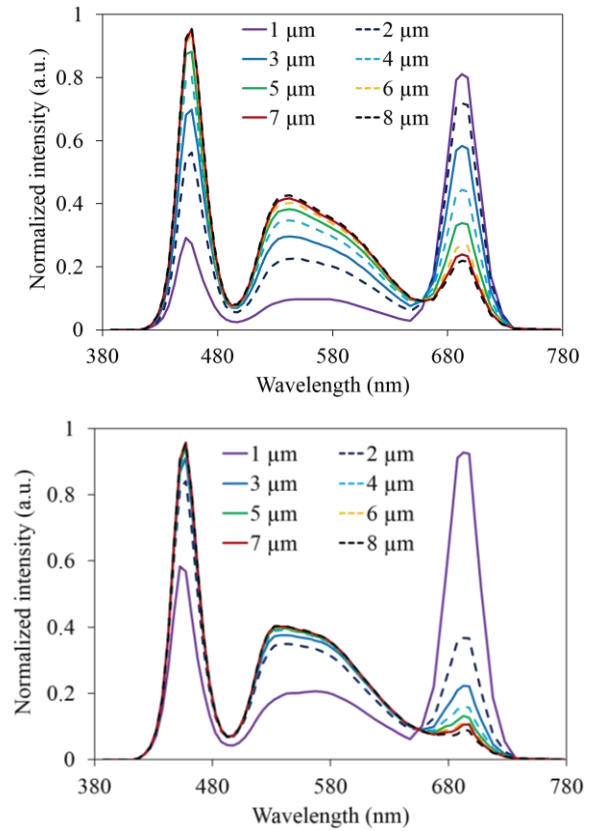


Fig. 6. The emission spectra of phosphor configurations as a function of $\text{Sr}_w\text{F}_x\text{B}_y\text{O}_z:\text{Eu}^{2+},\text{Sm}^{2+}$ size: (top) CPC and (bottom) IPC

A more important detection from the result in Fig. 6 is that the emission spectra of IPC makes less reduction than the one of CPC in the wavelength band of blue-light and the yellow-light. This implies that the luminous efficacy of IPC should be less decreased when the $\text{Sr}_w\text{F}_x\text{B}_y\text{O}_z:\text{Eu}^{2+},\text{Sm}^{2+}$ size is decreased. This plays a key role for interpreting the impact of $\text{Sr}_w\text{F}_x\text{B}_y\text{O}_z:\text{Eu}^{2+},\text{Sm}^{2+}$ size on the luminous efficacy. Indeed, the obtained result demonstrates that the spectrum region of red-light can be extended after mixing $\text{Sr}_w\text{F}_x\text{B}_y\text{O}_z:\text{Eu}^{2+},\text{Sm}^{2+}$ particles with the original phosphor compound, resulting in the improvement in color quality scale of WLEDs.

As the $\text{Sr}_w\text{F}_x\text{B}_y\text{O}_z:\text{Eu}^{2+},\text{Sm}^{2+}$ particles size continuously increases from 1 μm to 8 μm , the composite becomes more and more transparent in observable light, and that leads to scatter and absorb worse, as well as the increasing of LE and the decreasing CQS. According to (1), the transmitted light power grows exponentially with the decreasing of the extinction coefficient, which is a direct result from the enlargement of $\text{Sr}_w\text{F}_x\text{B}_y\text{O}_z:\text{Eu}^{2+},\text{Sm}^{2+}$ particle size. Reversely, the extinction coefficient tends to increase at higher $\text{Sr}_w\text{F}_x\text{B}_y\text{O}_z:\text{Eu}^{2+},\text{Sm}^{2+}$ concentration, which regards to the reduction of the transmitted light power I . This can be caused by the excessive addition of $\text{Sr}_w\text{F}_x\text{B}_y\text{O}_z:\text{Eu}^{2+},\text{Sm}^{2+}$ to the phosphor compounds, causing in the abundant enhancement of red-light spectrum region. Meanwhile, the blue-light and yellow-green light spectra decrease significantly irrespective of CPC, IPC.

Consequently, the lower luminous output is emitted in comparison with non- $\text{Sr}_w\text{F}_x\text{B}_y\text{O}_z:\text{Eu}^{2+}, \text{Sm}^{2+}$.

4. Conclusions

In this paper, we investigated the relationship between the key performance factors of WLEDs, namely CQS and LE, as well as the size and concentration of $\text{Sr}_w\text{F}_x\text{B}_y\text{O}_z:\text{Eu}^{2+}, \text{Sm}^{2+}$ for two configurations, i.e., CPC and IPC. The obtained results indicate that the size and concentration of $\text{Sr}_w\text{F}_x\text{B}_y\text{O}_z:\text{Eu}^{2+}, \text{Sm}^{2+}$ have contrary effects on the CQS. In fact, the CQS value grows with the increasing of $\text{Sr}_w\text{F}_x\text{B}_y\text{O}_z:\text{Eu}^{2+}, \text{Sm}^{2+}$ concentration but being reduced with the increasing of $\text{Sr}_w\text{F}_x\text{B}_y\text{O}_z:\text{Eu}^{2+}, \text{Sm}^{2+}$ size. This leads to the existence of an optimal point, where CQS values can exceed 76 for CPC. Specifically, the $\text{Sr}_w\text{F}_x\text{B}_y\text{O}_z:\text{Eu}^{2+}, \text{Sm}^{2+}$ size in 1-4 μm region presents more CQS than that in 5-8 μm in defiance of the increase in $\text{Sr}_w\text{F}_x\text{B}_y\text{O}_z:\text{Eu}^{2+}, \text{Sm}^{2+}$ concentration. Oppositely, the lower LE occurs in 1-4 μm region in comparison with 5-8 μm region. Moreover, if the $\text{Sr}_w\text{F}_x\text{B}_y\text{O}_z:\text{Eu}^{2+}, \text{Sm}^{2+}$ concentration is more inserted LE should be significantly decreased. This reduction is proved by following Lambert-Beer law and Mie-scattering theory. Through the analysis, it is considered that the size and concentration of $\text{Sr}_w\text{F}_x\text{B}_y\text{O}_z:\text{Eu}^{2+}, \text{Sm}^{2+}$ should be precisely controlled to maintain the LE to improve the CQS.

Acknowledgements

This research is funded by Foundation for Science and Technology Development of Ton Duc Thang University (FOSTECT), website: <http://fostect.tdtu.edu.vn>, under Grant FOSTECT.2017.BR.06.

References

- [1] J. -H. Li, J. Yan, D.-W. Wen, W. U. Khan, J. -X. Shi, M. -M. Wu, Q. Sua, P. A. Tannerb, *J. Mater. Chem. C* **4**, 8611 (2016).
- [2] D. -W. Wen, J. -J. Feng, J. -H. Li, J. -X. Shi, M. -M. Wu, Q. Su, *J. Mater. Chem. C* **3**, 2107 (2015).
- [3] Z. -G. Xia, Z. -H. Xu, M. -Y. Chen, Q. -L. Liu, *Dalton Trans.* **45**, 11214 (2016).
- [4] Z. -G. Xia, Q. -L. Liu, *Prog. Mater. Sci.* **84**, 59 (2016).
- [5] Z. Zhou, S. Q. Liu, Y. N. Liu, F. C. Wang, Z. X. He, Z. W. Tian, *Mater. Res. Innov.* **17**, 453 (2013).
- [6] S. Markus, T. Rosenthal, O. Oeckler, W. Schnick, *Crit. Rev. Solid State Mater. Sci.* **39**, 215 (2014).
- [7] L. Bin, J. -G. Li, Y. Sakka, *Sci. Technol. Adv. Mater.* **14**, 1 (2013).
- [8] H. Yu, W. W. Zi, S. Lan, H. F. Zou, S. C. Gan, X. C. Xu, G. Y. Hong, *Mater. Res. Innov.* **16**, 298 (2012).
- [9] N. D. Q. Anh, H. Y. Lee, T. T. Phuong, N. H. K. Nhan, T. H. Q. Minh, T. H. Ly, *J. Chin. Ins. Eng.* **40**, 1 (2017).
- [10] P. C. Hung, J. Y. Tsao, *J. Disp. Technol.* **9**, 405 (2013).
- [11] J. -M. Choi, S. S. Kim, S. -P. Chang, *Adv. Appl. Ceram.* **115**, 210 (2016).
- [12] J. J. Zhang, R. Hu, X. J. Yu, B. Xie, X. B. Luo, *Optics & Laser Technology* **88**, 161 (2017).
- [13] W. M. Yen, M. J. Weber, *Inorganic Phosphors: Compositions, Preparation and Optical Properties* CRC Press, Florida, 2004.
- [14] R. Stefani, A. D. Maia, E. E. S. Teotonio, M. A. F. Monteiro, M. C. F. C. Felinto, H. F. Brito, *J. Solid State Chem.* **179**, 1086 (2006).
- [15] K. Jang, I. Kim, S. T. Park, Y. L. Huang, H. J. Seo, C. D. Kim, *J. Phys. Chem. Solids* **67**, 2316 (2006).
- [16] R. Komatsu, H. Kawano, Z. Oumar, K. Shinoda, V. Petrov, *J. Crystal Growth* **275**, e843 (2005).
- [17] Q. H. Zeng, Z. W. Pei, S. B. Wang, Q. Su, *Spectrosc. Lett.* **32**, 895 (1999).
- [18] Z. -Y. Liu, S. Liu, K. Wang, X.-B. Luo, *Appl. Opt.* **49**, 247 (2010).

*Corresponding author: leehy@mail.ee.kuas.edu.tw
nguyendoanquocanh@tdt.edu.vn
phanxuanle.ts@gmail.com